Cancer Cell
Article

Growth Factor Independence 1 Antagonizes a p53-Induced DNA Damage Response Pathway in Lymphoblastic Leukemia

Cyrus Khandanpour,[1,3,9] James D. Phelan,[4,9,10] Lothar Vassen,[1] Judith Schütte,[6] Riyan Chen,[1] Shane R. Horman,[4,11] Marie-Claude Gaudreau,[1,2] Joseph Krongold,[1,7] Jinfang Zhu,[8] William E. Paul,[8] Ulrich Dührsen,[3] Bertie Göttgens,[6] H. Leighton Grimes,[4,5,*] and Tarik Möröy[1,2,7,*]

[1]Institut de recherches cliniques de Montréal (IRCM), 110 Avenue des Pins Ouest, Montréal, Quebec H2W 1R7, Canada
[2]Département de Microbiologie et Immunologie, Université de Montréal, Montréal, Québec H3C 3J7, Canada
[3]Department of Haematology, University Hospital, University Duisburg-Essen, Hufelandstrasse 55, 45122 Essen, Germany
[4]Division of Cellular and Molecular Immunology
[5]Division of Experimental Hematology
Cincinnati Children's Hospital Medical Center, Cincinnati, OH 45229, USA
[6]Cambridge Institute for Medical Research and Wellcome Trust-Medical Research Council Cambridge Stem Cell Institute, University of Cambridge, Cambridge CB2 0XY, UK
[7]Division of Experimental Medicine, McGill University, Montreal, Québec H3A 1A3, Canada
[8]Laboratory of Immunology, National Institute of Allergy and Infectious Disease, National Institutes of Health, Bethesda, MD 20829, USA
[9]These authors contributed equally to this work
[10]Present address: Metabolism Branch, Center for Cancer Research, National Cancer Institute, National Institutes of Health, Bethesda, MD 20892, USA
[11]Present address: Genomics Institute of the Novartis Research Foundation, San Diego, CA 92121, USA
*Correspondence: lee.grimes@cchmc.org (H.L.G.), tarik.moroy@ircm.qc.ca (T.M.)
http://dx.doi.org/10.1016/j.ccr.2013.01.011

SUMMARY

Most patients with acute lymphoblastic leukemia (ALL) fail current treatments highlighting the need for better therapies. Because oncogenic signaling activates a p53-dependent DNA damage response and apoptosis, leukemic cells must devise appropriate countermeasures. We show here that growth factor independence 1 (Gfi1) can serve such a function because Gfi1 ablation exacerbates p53 responses and lowers the threshold for p53-induced cell death. Specifically, Gfi1 restricts p53 activity and expression of proapoptotic p53 targets such as *Bax*, *Noxa (Pmaip1)*, and *Puma (Bbc3)*. Subsequently, Gfi1 ablation cures mice from leukemia and limits the expansion of primary human T-ALL xenografts in mice. This suggests that targeting Gfi1 could improve the prognosis of patients with T-ALL or other lymphoid leukemias.

INTRODUCTION

Many patients with acute lymphoblastic leukemia (ALL) and lymphoma die of tumor relapse (Gökbuget and Hoelzer, 2009). Experiments with mouse models have shown that T-ALL-like diseases can be accelerated by the overexpression of the transcriptional repressor growth factor independence 1 (Gfi1), which is a well-established nuclear zinc finger protein and regulator of lymphoid development (Gilks et al., 1993; Zörnig et al., 1996; Li et al., 2010; Pargmann et al., 2007; Spooner et al., 2009; Yücel et al., 2003). Germline *Gfi1* deletion in mice modestly reduces thymic cellularity, with an accumulation of cells between double-negative 1 (DN1) and DN2 stages as well as a skew from $CD4^+$ to $CD8^+$ (Yücel et al., 2003). In contrast, the thymus is

Significance

Chemotherapy is nonspecific and highly toxic, damaging both host and tumor tissues. Even when effective, patients suffer dramatic side effects from standard treatments. Molecular-based targeted therapies have shown great promise but lack broad applicability due to the heterogeneity of oncogenic pathways mutated during transformation. Here, we demonstrate that ablation of Gfi1 broadly leads to lymphoid tumor regression and host survival independent of the transforming pathway. We demonstrate that Gfi1 limits the proapoptotic functions of the endogenous gatekeeper p53. Gfi1 inhibition amplifies p53-dependent proapoptotic responses driven by oncogenic stress; consequently, transformed lymphoid tissues are uniquely susceptible to Gfi1 inhibition. Thus, in combination with current therapies, Gfi1 inhibition may allow the use of lower cytotoxic doses, which would benefit patients directly.

relatively normal when *Gfi1* is deleted after the DN stage (Zhu et al., 2006), which suggests that Gfi1 mainly acts during early steps of T lymphopoiesis. Gfi1's ability to accelerate leukemogenesis in mice and its function in lymphoid development prompted us to explore the role of Gfi1 ablation in the initiation or maintenance of lymphoid malignancies.

RESULTS

GFI1 Is Associated with a Subgroup of Human T-ALL and Accelerates NOTCH1-Induced T-ALL in Mice

Although the oncogenic impact of high-level Gfi1 expression in murine T cell leukemogenesis is well established, an association of *GFI1* with human T-ALL has not been clearly shown. Because over 50% of human T-ALL displays mutated *NOTCH1* (Weng et al., 2004) or Notch1 regulatory proteins (O'Neil et al., 2007; Thompson et al., 2007) resulting in overexpression of Notch1 target genes (Palomero et al., 2006; Sharma et al., 2006; Weng et al., 2006), we performed hierarchical clustering of microarray data from independent cohorts of patients with T-ALL using *NOTCH1* mutation status (Ferrando et al., 2002), Notch1 target gene activation (Palomero et al., 2006; Van Vlierberghe et al., 2008), or early T cell precursor (ETP)-ALL diagnosis (Coustan-Smith et al., 2009) and examined *GFI1* expression (Figures 1A and 1B; Figures S1A–S1F available online).

We observed that patients with ETP-ALL had low levels of *GFI1* expression compared to those with a positive *NOTCH1* signature (Figures 1B, S1D, and S1E), suggesting a functional role for Gfi1 in *NOTCH1*-dependent human T-ALL. However, *GFI1* is unlikely a Notch1 target because intracellular Notch1 (ICN) does not occupy the *GFI1* locus nor was *GFI1* expression altered by γ-secretase inhibitors (GSIs) based on our own results as well as published data (Figure S1F) (Margolin et al., 2009; Medyouf et al., 2011). Also, we can show that mice transplanted with bone marrow (BM) cells overexpressing ICN and Gfi1 developed leukemia faster than mice transplanted with cells only overexpressing ICN (Figures S1G–S1I), corroborating previous reports on the function of Gfi1 in T cell leukemogenesis (Schmidt et al., 1998; Zörnig et al., 1996) and extending it to human ICN-mediated T-ALL.

Gfi1 Deletion Delays the Development of T-ALL

To test whether ablation of Gfi1 could inhibit the onset of T-ALL, we used five different mouse models, in which we could temporally delete *Gfi1*. First, we transplanted ICN-expressing BM cells from mice carrying a tamoxifen (OHT)-inducible *Rosa26* Cre-recombinase transgene (Cre^{ERT2}) (Hameyer et al., 2007) enabling inducible deletion of floxed *Gfi1* alleles ($Gfi1^{f/f}$) (Horman et al., 2009; Velu et al., 2009) (Figure 1C). Although vehicle-treated animals died within 66 days, OHT-treated recipients developed leukemia within 87 days with similar T-ALL characteristics (Figures 1C–1F). However, all tumors emerging after OHT treatment had intact *Gfi1* alleles (Figure 1D), suggesting that ICN-induced T-ALL selects for Gfi1.

To confirm this, we used a T cell-specific Cre transgene ($LckCre^{+}$) and $Gfi1^{f/\Delta}$ transgenic mice, in which *Rosa26* locus-mediated expression of ICN and EGFP is blocked by a floxed STOP cassette ($Rosa\ ICN^{LSL}$) (Murtaugh et al., 2003). We injected these mice with N-ethyl-N-nitrosourea (ENU), which induces T cell leukemia and shortens the latency of leukemogenesis (Kundu et al., 2005; Yuan et al., 2001). Approximately 50% of all tumors arising in $LckCre^{+}$;$Rosa\ ICN^{LSL}$;$Gfi1^{+/+}$ mice were $EGFP^{+}$ (i.e., expressing ICN and Gfi1, Figures S1J and S1K). However, ENU-induced tumors that arose in $LckCre^{+}$;$Rosa\ ICN^{LSL}$;$Gfi1^{f/\Delta}$ mice were always $EGFP^{-}$ (i.e., ICN^{-} and Gfi1 wild-type, Figure S1K,), also suggesting that ICN-mediated tumorigenesis selects for Gfi1. In yet another Notch-driven leukemogenesis model, in which constitutive absence of *Gfi1* was coupled with a *CD4* promoter-driven mutant Notch1 transgene ($Notch1^{\Delta CT}$; Priceputu et al., 2006), T-ALL development was substantially decreased and delayed (Figures 1G–1I).

To explore the impact of *Gfi1* loss in mouse models of T-ALL that are not initiated by Notch, we either infected $Gfi1^{+/+}$ and $Gfi1^{-/-}$ newborn mice with Murine Moloney Leukemia (MMLV) (Scheijen et al., 1997) or injected adolescent mice with ENU. All MMLV-infected $Gfi1^{+/+}$ mice developed lymphoid malignancies, whereas only 40% of MMLV-infected $Gfi1^{-/-}$ mice did. The remaining mice were censored due to neurological problems consistent with reports on older $Gfi1^{-/-}$ mice (unpublished data). Notably, $Gfi1^{-/-}$ lymphoid malignancies were significantly less robust than $Gfi1^{+/+}$ tumors (Figures 1J–1L). Similarly, >85% of the ENU-injected $Gfi1^{+/+}$ mice, but only 20% of $Gfi1^{-/-}$ mice, developed T cell leukemia (Figure S1L); the remaining mice succumbed to ENU-induced toxicity. As in other models, ENU-initiated $Gfi1^{-/-}$ tumors developed slower and were significantly less robust than $Gfi1^{+/+}$ tumors (Figures S1L–S1N). Neither $Gfi1^{+/+}$ nor $Gfi1^{-/-}$ ENU-induced tumors were found to harbor *Notch1* mutations in the HD or PEST domain (Table S1). Thus, results from these five independent T-ALL models, initiated by various oncogenic pathways, led us to conclude that ablation of *Gfi1* delays, impedes, or is counterselected during T-ALL formation.

T-ALL Disease Maintenance Is Gfi1 Dependent

$Mx1\text{-}Cre^{+}$;$Gfi1^{f/f}$ or $Gfi1^{f/f}$ mice were treated with ENU to elicit T cell leukemia. After 50 days, both groups were injected with pIpC (Horman et al., 2009). All $Gfi1^{f/f}$ mice developed T-ALL, but $Mx1\text{-}Cre^{+}$;$Gfi1^{f/f}$ mice separated into two different subgroups following pIpC injection. One subgroup remained healthy until the study was terminated (Figure 2A, $Mx1\text{-}Cre^{+}$;$Gfi1^{f/f}$, full excision) or died of ENU toxicity. The second subgroup displayed partial *Gfi1* deletion and succumbed to T cell leukemia similar to ENU/pIpC-treated $Gfi1^{f/f}$ mice (Figure 2A, $Mx1\text{-}Cre^{+}$;$Gfi1^{f/f}$ partial excision).

To investigate whether loss of *Gfi1* was causing tumor regression or preventing tumor formation, we used ultrasound imaging. Upon detection of a tumor (Figure 2B), *Gfi1* deletion was induced with pIpC. All ENU-induced tumors in $Gfi1^{f/f}$ mice clearly showed increases in tumor size, whereas tumors that developed in $Mx1\text{-}Cre^{+}$;$Gfi1^{f/f}$ animals showed variable changes in size (Figures 2C and S2A). Following pIpC injection, disease-free survival, tumor growth, and blast cell detection all directly correlated with the degree of *Gfi1* deletion in the tumor (Figures 2B, 2C, and S2B) because we found that *Gfi1* deletion was incomplete in tumors that progressed but was complete in tumors that regressed (Figure S2A).

We verified this observation in a second T-ALL model, in which disease was induced by Notch1 activation and

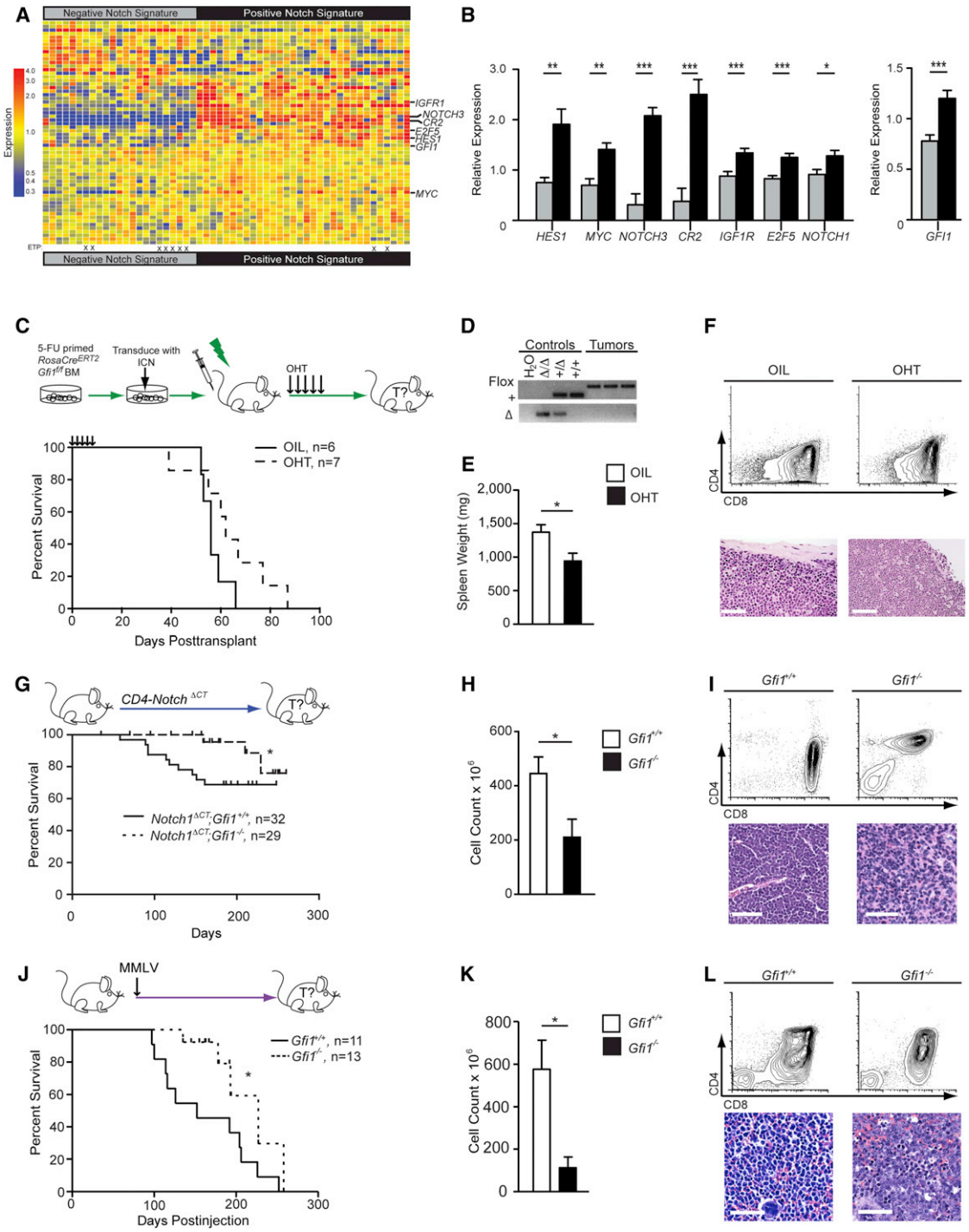

Figure 1. Gfi1 Associates with NOTCH1 in Human T-ALL, and Deletion Delays the Development of Disease

(A) Heatmap of expression of published Notch1 target genes used to classify gene expression array data from 55 patients with T-ALL (GSE8879) into two groups: "Negative Notch Signature" (left), and "Positive Notch Signature" (right). ETP-ALL diagnosis is designated by an "X."

(B) Quantification of relative expression of *NOTCH1*, *GFI1*, and Notch1 target genes *HES1*, *MYC*, *NOTCH3*, *CR2*, *IGF1R*, and *E2F5* in 55 patients with T-ALL with either a "Negative Notch Signature" (gray) or a "Positive Notch Signature" (black).

(C) Top view shows *RosaCre*^{ERT2};*Gfi1*$^{f/f}$ BM cells that were transduced with vectors expressing ICN and then transplanted. Mice were given vehicle or tamoxifen to induce Cre activity. Bottom view is a Kaplan-Meier curve.

(D) PCR genotype analysis of the *Gfi1* locus in control tissues (*Gfi1*$^{\Delta/\Delta}$, *Gfi1*$^{+/\Delta}$, *Gfi1*$^{+/+}$) and in representative tumors from mice either treated with vehicle or OHT. FLOX, *Gfi1*^{f} allele; +, the wild-type allele; Δ, deleted allele.

(E and F) Spleen weights (E; n = 6 each group) and flow cytometric analysis of thymic tumors (F, top panels) and spleen sections with H&E (F, bottom panels) collected during postmortems from indicated transplant groups.

(legend continued on next page)

accelerated by ENU injection. Mice were monitored by ultrasound and upon tumor detection, treated with pIpC (Figure 2D). Although all pIpC-injected *Notch1*$^{\Delta CT}$;*Gfi1*$^{f/f}$ mice died, all pIpC-injected *Notch1*$^{\Delta CT}$;*Mx1-Cre*$^{+}$;*Gfi1*$^{f/f}$ tumors with complete deletion of *Gfi1* regressed, and the mice survived (Figures 2D–2F). This regression also correlated with lower numbers of blast cells in the blood of pIpC-treated *Notch1*$^{\Delta CT}$;*Mx1-Cre*$^{+}$;*Gfi1*$^{f/f}$ mice compared to *Notch1*$^{\Delta CT}$;*Gfi1*$^{f/f}$ controls (Figure S2C).

Next, *Gfi1*$^{f/f}$ or *Mx1-Cre*$^{+}$;*Gfi1*$^{f/\Delta}$ tumor cells were transplanted into syngeneic recipients. In recipients that did not receive pIpC, only tumors with an intact floxed *Gfi1* allele emerged (data not shown). However, when recipient mice were treated with pIpC, all mice that received *Gfi1*$^{f/f}$ tumors died, whereas mice receiving *Mx1-Cre*$^{+}$;*Gfi1*$^{f/\Delta}$ tumors survived tumor free (Figure 2G). To demonstrate that loss of *Gfi1* specifically leads to tumor regression in a cell-autonomous manner, we inhibited Gfi1 function in three Tal1-transformed murine T-ALL cell lines (Cullion et al., 2009) by overexpressing a dsRed-marked Gfi1 dominant-negative mutant (Gfi1^{N382S}) (Horman et al., 2009; Person et al., 2003; Zarebski et al., 2008). Two days after the initial measurement of transduction, and in contrast to empty vector-transduced cells, only 15%–20% of cells transduced with dsRed^{+} Gfi1^{N382S}-expressing vectors were still dsRed^{+} (Figure 2H).

To determine the clinical potential of targeting Gfi1, we injected *Gfi1*$^{f/f}$ and *Mx1-Cre*$^{+}$;*Gfi1*$^{f/f}$ mice (CD45.2^{+}) with ENU, waited 50 days to allow tumor initiation, and then treated with pIpC to delete *Gfi1*. Four weeks after the first pIpC injection, both groups of mice were sublethally irradiated and transplanted with syngenic CD45.1^{+} BM cells (BMT) to prevent BM failure associated with ENU (Figures 2I and 2J). The combination therapy was not sufficient to cure the mice of T-ALL because 80% of ENU-treated *Gfi1*$^{f/f}$ mice still succumbed to disease (one died of nontumor-related reasons). However, when therapy was combined with *Gfi1* deletion, complete tumor remission was observed in every transplant recipient (Figures 2I and 2J). Taken together, our data strongly implicate Gfi1 in the maintenance of established T cell malignancies, their ability to kill secondary hosts, and potentially in improving therapy.

Maintenance of B Cell Lymphoma Is Dependent on Gfi1

To test whether other lymphoid malignancies were also dependent on Gfi1, we used *Eμ-Myc* transgenic mice, which develop clonal B cell lymphomas (Adams et al., 1985). Loss of *Gfi1* did not affect the latency, incidence, or pathology of tumor initiation (Figures 3A and 3B) but completely blocked the ability of lymphoma to kill secondary recipients (Figure S3A). Thus, similar to the T cell models, Gfi1 is required for robust tumorigenesis. To determine whether Gfi1 is required for B cell lymphoma maintenance, we used an inducible model (Zhu et al., 2006) to delete *Gfi1*$^{f/f}$ after a lymphoma had formed. Although pIpC injection had no effect on progression of disease in *Gfi1*$^{f/f}$;*Eμ-Myc* mice, it led to tumor regression and a significant reduction of leukemic blasts in the peripheral blood of *Mx1-Cre*;*Gfi1*$^{f/f}$;*Eμ-Myc* mice (Figures 3C–3E and S3B), suggesting that Gfi1 is indeed necessary to maintain a B cell lymphoma. Similar to the results with our T-ALL models, loss of *Gfi1* significantly improved the outcome of *Gfi1*$^{-/-}$;*Eμ-Myc* mice treated with sublethal irradiation and BMT after detection of a tumor, whereas *Gfi1*$^{+/+}$;*Eμ-Myc* animals died of tumor relapse (Figure 3F). These data suggest that targeting Gfi1 could also be beneficial for treating B cell lymphoma.

Gfi1 Integrates the Cellular Transcriptional Response to DNA Damage/p53 Induction

To investigate how loss of Gfi1 induces tumor regression, we compared gene expression profiles of T cell leukemia from two different models (Figures 2A and 2D) upon inducible deletion of *Gfi1* (Figure 4A). Gene Set Enrichment Analysis (GSEA) (Subramanian et al., 2005) demonstrated significant deregulation of multiple key leukemic pathways, including cell-cycle progression, NFκB signaling, and basal transcription among others (Table S2; data not shown). Normal thymocytes do not disappear upon loss of Gfi1 as the tumors do. Therefore, to identify mechanisms that might explain tumor regression, we focused on those pathways that were similarly deregulated in both ENU and *Notch1*$^{\Delta CT}$-induced tumors from *Gfi1*$^{-/-}$ and *Gfi1*$^{+/+}$ mice but were not enriched in normal nonmalignant *Gfi1*$^{-/-}$ versus *Gfi1*$^{+/+}$ thymocytes. We noticed a striking number of shared GSEA signatures that included deregulated p53 signaling, DNA damage/repair pathways, and a proapoptotic response (Figures 4B and 4C; Table S2), suggesting that an accelerated cell death program might be initiated in tumor cells that lack Gfi1.

An emerging concept proposes that oncogenic signaling induces uncoordinated cell division, generating collapsed replication forks and DNA double-strand breaks, which in turn initiate a DNA damage response, activating p53 and inducing apoptosis. Therefore, tumor cells must counteract cell death in order to survive (Bartek et al., 2007; Bartkova et al., 2007; Di Micco et al., 2006; Halazonetis et al., 2008). In agreement with this theory, leukemic cells from our tumor models displayed increased levels of phosphorylated H2AX (γH2AX), indicating DNA double-strand breaks, and higher levels of spontaneous

(G) Top view shows *Notch1*$^{\Delta CT}$;*Gfi1*$^{+/+}$ and *Notch1*$^{\Delta CT}$;*Gfi1*$^{-/-}$ mice that were monitored for tumor development and survival. Bottom view is a Kaplan-Meier curve.

(H and I) Spleen weights (H) and flow cytometric analysis (I, top panels) and histological sections (I, bottom panels) of *Notch1*$^{\Delta CT}$;*Gfi1*$^{+/+}$ (n = 7) and *Notch1*$^{\Delta CT}$;*Gfi1*$^{-/-}$ (n = 3) tumors.

(J) Top view shows *Gfi1*$^{+/+}$ and *Gfi1*$^{-/-}$ newborn mice that were injected with MMLV. Bottom view is a Kaplan-Meier curve.

(K) Thymic tumor cell numbers of *Notch1*$^{\Delta CT}$-induced tumors.

(L) Flow cytometric analysis (top panels) and histological section (bottom panels) of MMLV-induced *Gfi1*$^{+/+}$ versus *Gfi1*$^{-/-}$ tumors.

Scale bars, 50 μm. Vertical line (|) in all Kaplan-Meier curves indicates censored mice. Mean and mean ± SEM are shown unless stated otherwise. *p < 0.05, **p < 0.01, ***p < 0.001.

See also Figure S1 and Table S1.

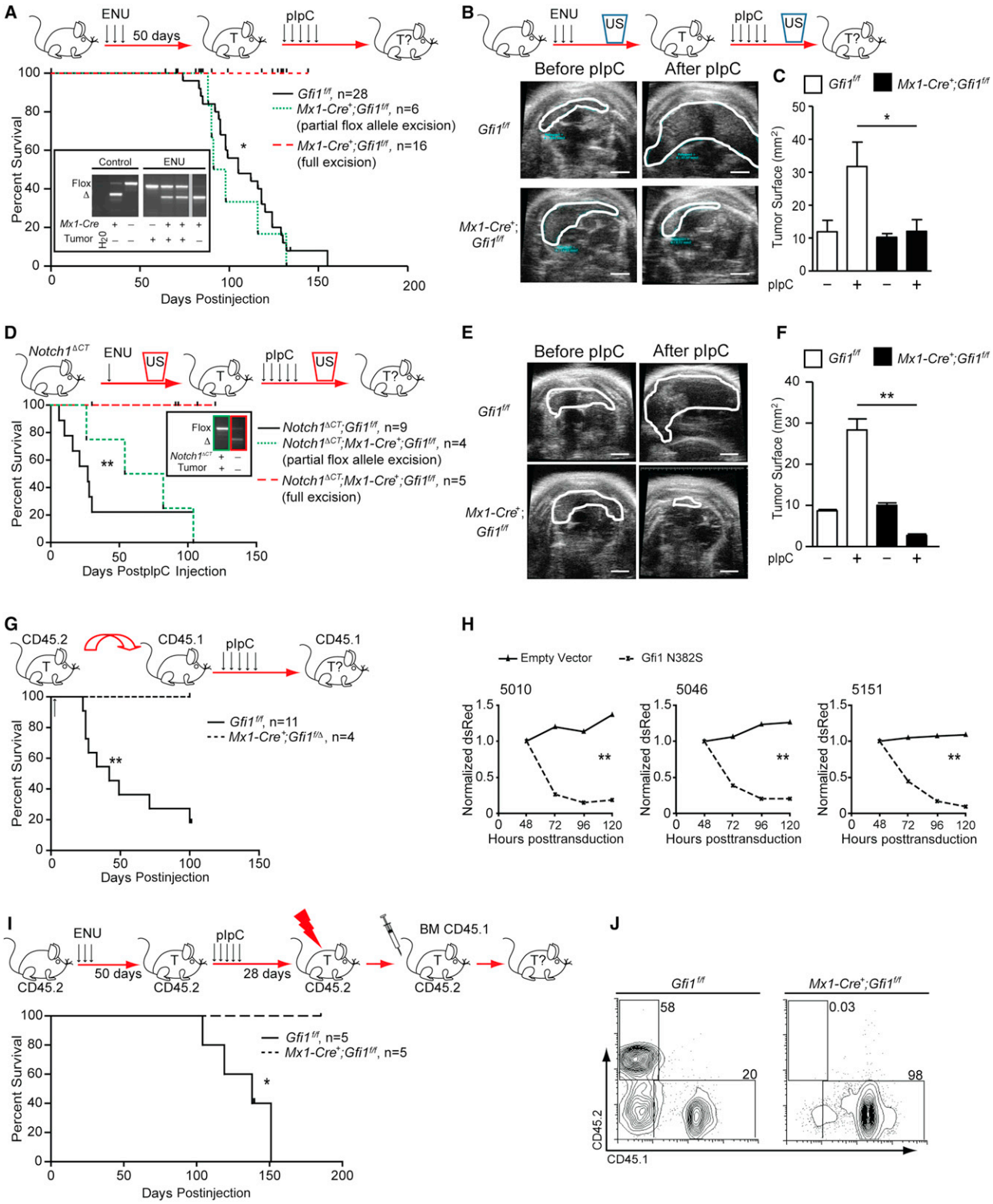

Figure 2. Gfi1 Is Required for T Cell Leukemia Maintenance

(A) Top view shows *Gfi1*$^{f/f}$ or *Mx1-Cre*$^{+}$;*Gfi1*$^{f/f}$ mice that were treated with ENU and subsequently with pIpC. Bottom view is a Kaplan-Meier curve. Inset presents PCR analysis of the *Gfi1* locus in control tissues and in representative tumors (T) for *Gfi1* flox and excised (Δ) alleles.

(B) Top view shows *Gfi1*$^{f/f}$ or *Mx1-Cre*$^{+}$;*Gfi1*$^{f/f}$ mice that were treated with ENU and followed for tumors by ultrasound (US). Next, mice were treated with pIpC, and tumor development was determined by ultrasound. Bottom view is representative ultrasound images. Scale bars, 20 mm.

(legend continued on next page)

apoptosis than untransformed thymocytes (Figures 4D–4F). We also noted that the number of apoptotic cells was further increased in those tumors where *Gfi1* was inducibly deleted (Figure 4F). Additionally, when we irradiated $Gfi1^{-/-}$ leukemic cells, we observed decreased survival compared to $Gfi1^{+/+}$ tumors (Figures 4G). Finally, when we overexpressed Bcl2 in Tal1-transformed T cell lines, counterselection of the dominant-negative mutant $Gfi1^{N382S}$ was either absent or delayed (compare Figure 4H to Figure 2H). These data demonstrate that Gfi1 is required in lymphoid tumors to counter DNA damage-induced death and suggest that DNA damage/p53-induced signals are dominant effectors of *Gfi1* loss-of-function apoptotic phenotypes in T-ALL.

In contrast to *Gfi1*-deleted tumors, $Gfi1^{-/-}$ thymocytes display only mildly increased levels of apoptosis of c-Kit^{+} subsets (compared to $Gfi1^{+/+}$) (Yücel et al., 2003). In agreement with this observation, we noted that whereas GSEA of gene expression data of $Gfi1^{-/-}$ versus $Gfi1^{+/+}$thymocytes is enriched for apoptotic signatures, the DNA damage and p53 signatures, which drive the execution of apoptosis, were not enriched (Figures 5A and 5B). Thus, we hypothesized that the introduction of a DNA damage signal (inherent to tumors) to $Gfi1^{-/-}$ thymocytes may elicit the same increased apoptotic phenotype in thymocytes that was found in tumors. Indeed, gene expression analysis revealed that a comparison between γ-irradiated (to induce DNA damage) $Gfi1^{-/-}$ versus $Gfi1^{+/+}$thymocytes recapitulated the exaggerated $Gfi1^{-/-}$ GSEA DNA damage and p53 signatures found in leukemia cells (compare Figures 4B and 5B). Moreover, DNA damage induced by daunorubicin, etoposide, or by various doses of γ irradiation resulted in significantly decreased $Gfi1^{-/-}$ thymocyte survival and mitochondrial potential (Figures S4A–S4E). Although $Gfi1^{-/-}$ thymocytes showed similar levels of γH2AX, p53 induction, and p53 phosphorylation compared to $Gfi1^{+/+}$ controls (Figures S4F and S4G), $Gfi1^{-/-}$ thymocytes displayed increased cleaved caspase-3 and PARP (Figures S4H and S4I). These data indicate that Gfi1 antagonizes DNA damage-induced apoptotic pathways downstream of DNA damage detection but upstream of caspase and PARP1 cleavage.

To analyze this in more detail, the expression of cell death-associated p53 targets such as *Bax*, *Pmaip1* (Noxa), and *Bbc3* (Puma) was tested and found to be further induced in irradiated $Gfi1^{-/-}$ thymocytes compared to $Gfi1^{+/+}$ controls (Figure 5C). These genes appear to be direct Gfi1 targets because interrogation of Gfi1 ChIP-seq data showed enriched Gfi1 binding in the regulatory regions of *Bax*, *Pmaip1*, and *Bbc3* compared to IgG controls (Figure 5D). These data suggest that Gfi1 co-occupies p53-responsive genes and regulates their expression. Interestingly, significant p53 binding to these same Gfi1-bound regions within the promoters (underscored in Figure 5D) of *Bax*, *Pmaip1*, and *Bbc3* was observed in thymocytes after induction of p53 by irradiation (Figure 5E). To assess whether Gfi1 and p53 globally regulate the expression of proapoptotic p53 effector genes, we examined the leading edge of the GSEA $Gfi1^{-/-}$-irradiated thymocyte signature and found that >70% of the apoptotic genes were in fact proapoptotic effectors (Figure S4J). Moreover, combining the gene expression and ChIP-seq analyses revealed that Gfi1 occupies 55 of 77 p53-effector genes (>70%) deregulated in irradiated $Gfi1^{-/-}$ thymocytes (Figure 5F). We next validated the ChIP-seq data with ChIP-qPCR using primer sets for 14 of the 55 genes. These genes were (1) occupied by Gfi1 according to ChIP-seq data with reads over 100 compared to Ig controls, (2) at least 1.5-fold differentially expressed between $Gfi1^{-/-}$ and $Gfi1^{+/+}$ thymocytes after irradiation, and (3) known p53 effector genes according to empirically tested data in the Molecular Signature Database (MSigDB). ChIP-qPCR confirmed binding of Gfi1 in irradiated thymocytes with an enrichment of >1.5-fold in 10 of the 14 genes tested, suggested Gfi1 binding in 3 genes with an enrichment of 1.3–1.5, and demonstrated little to no binding in only 1 of the 14 primer sets tested (Figure S4K). Co-occupation of the same loci by Gfi1 and p53 was found in the majority of genes tested (9 of 14, Figure S4L). A time-dependent analysis on 4 of the 14 loci (*Bax*, *Pmaip1*, *Bbc3*, and *Cdkn1a)* revealed that a co-occupation by Gfi1 and p53 is maintained over time but that p53 occupation clearly dominates at 120 min after the initial DNA damage signal over Gfi1 (Figure S4M). This suggests that during the immediate response after DNA damage, Gfi1 and p53 coregulate target genes, but if the DNA damage signal persists, a p53-dominated regulation prevails.

We investigated the involvement of the p53-activated apoptosis pathway in $Gfi1^{-/-}$ thymocyte survival after DNA damage. To do so, we deleted *Trp53* or overexpressed *Bcl2* and found that either condition completely rescued the exaggerated $Gfi1^{-/-}$ thymocyte apoptosis upon DNA damage signaling (Figure 5G). Further investigation into the underlying

(C) Change of thymic surface area before and after treatment with pIpC for mice (see B).
(D) Top view shows $Notch1^{\Delta CT}$;$Gfi1^{f/f}$ or $Notch1^{\Delta CT}$;$Mx1\text{-}Cre^{+}$;$Gfi1^{f/f}$ mice that were treated with ENU and subsequently monitored by ultrasound for tumor (T) development. Upon appearance of a mass, mice were injected with pIpC and followed for tumor progression or regression by ultrasound. Bottom view is a Kaplan-Meier curve. Inset presents a PCR analysis of allele excision (Δ).
(E) Representative ultrasound images of tumors before and after pIpC injection. Scale bars, 20 mm.
(F) Change of thymic surface area before and after treatment with pIpC (see E).
(G) Top view shows $Gfi1^{f/f}$ tumors or tumors that had one *Gfi1* allele deleted ($Mx1\text{-}Cre^{+}$;$Gfi1^{f/\Delta}$) were transplanted into CD45.1 recipient mice, which were then treated with pIpC. Bottom view is a Kaplan-Meier curve.
(H) T-ALL cell lines 5151, 5046, and 5010 were transduced with retrovirus vectors expressing $Gfi1^{N382S}$ and dsRed or dsRed alone. dsRed was measured over time by FACS and normalized to the level at 48 hr. One of three representative experiments is shown.
(I) Top view shows $Gfi1^{f/f}$ or $Mx1\text{-}Cre^{+}$;$Gfi1^{f/f}$ mice that were injected with ENU. Fifty days later, they were treated with pIpC. Twenty-eight days later, they were irradiated, and transplanted with wild-type CD45.1 BM cells, then followed for survival. Bottom view is a Kaplan-Meier curve. One $Gfi1^{f/f}$ mouse was sacrificed for morbidity unrelated to leukemia.
(J) BM of mice in (I) at the end of observation was examined for contribution of the CD45.2 (host BM) and CD45.1 (donor BM).
Vertical line (|) in all Kaplan-Meier curves indicates censored mice. Mean and mean ± SEM are shown unless stated otherwise. *$p < 0.05$, **$p < 0.01$.
See also Figure S2.

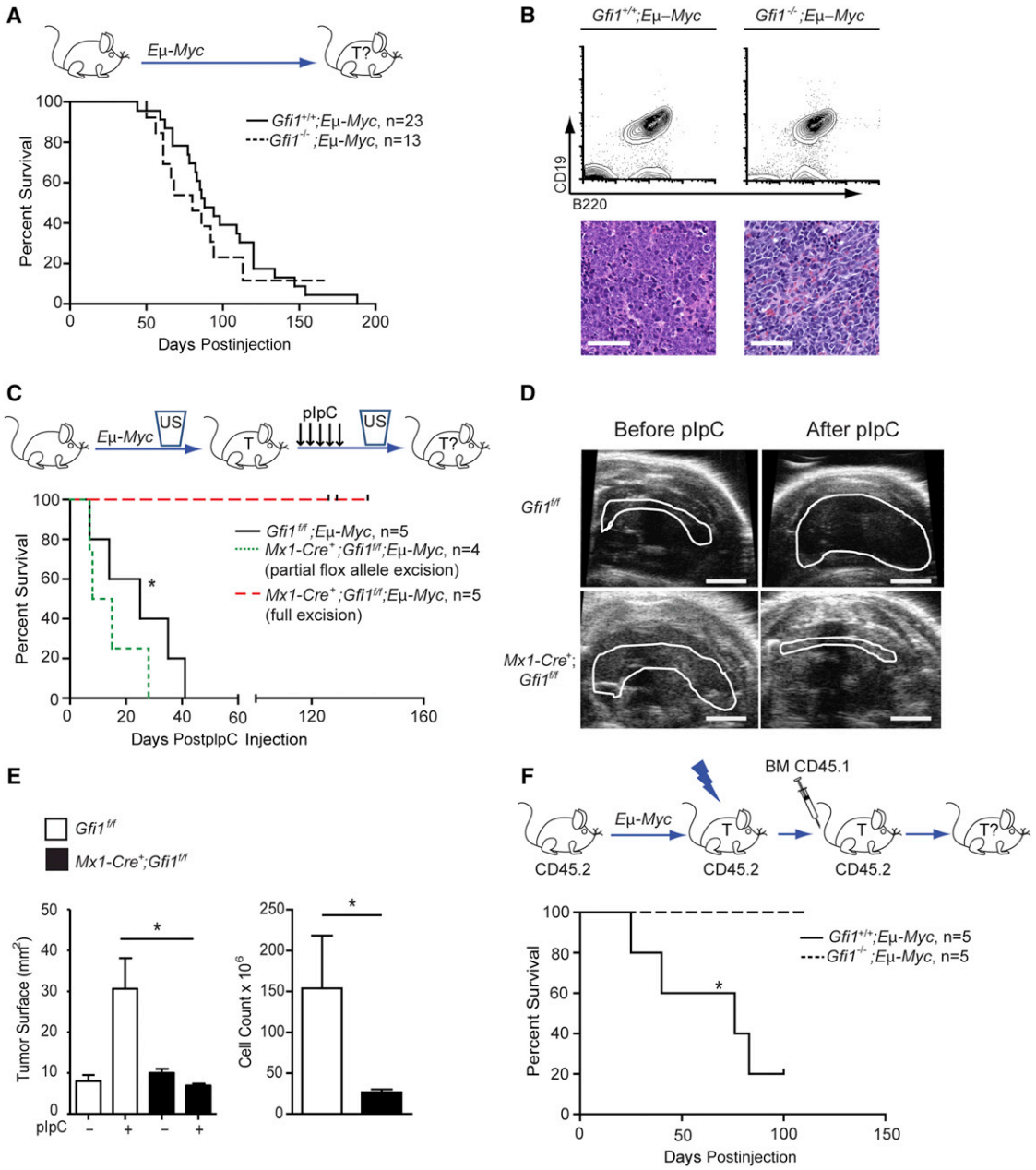

Figure 3. Gfi1 Is Required for Maintenance of B Cell Lymphoma

(A) Top view shows *Gfi1*$^{+/+}$;*Eμ-Myc* and *Gfi1*$^{-/-}$;*Eμ-Myc* mice that were monitored for tumor development and survival. Bottom view is a Kaplan-Meier curve.

(B) Flow cytometric analysis (top) and histological sections (bottom) of *Eμ-Myc*-induced *Gfi1*$^{+/+}$ and *Gfi1*$^{-/-}$ tumors. Scale bars, 50 μm.

(C) Top view shows *Mx1-Cre*$^{+}$;*Gfi1*$^{f/f}$;*Eμ-Myc* and *Gfi1*$^{f/f}$;*Eμ-Myc* mice that were observed by ultrasound for appearance of B cell lymphoma. Upon appearance of a mass, mice were injected with pIpC and monitored for tumor progression and survival. Bottom view is a Kaplan-Meier curve.

(D) Representative ultrasound images of tumors before and after pIpC injection. Scale bars, 20 mm.

(E) Change of tumor surface area (left) before and after treatment with pIpC for mice with the indicated genotypes as well as cellularity of mediastinal tumor after treatment (right).

(F) Top view shows *Gfi1*$^{+/+}$;*Eμ-Myc* and *Gfi1*$^{-/-}$;*Eμ-Myc* animals that were observed until enlarged lymph nodes evidenced tumor development, then they were irradiated and transplanted with CD45.1 BM cells and monitored for survival. Bottom view is a Kaplan-Meier curve.

Vertical line (|) in all Kaplan-Meier curves indicates censored mice. Mean and mean ± SEM are shown unless stated otherwise. *$p < 0.05$.

See also Figure S3.

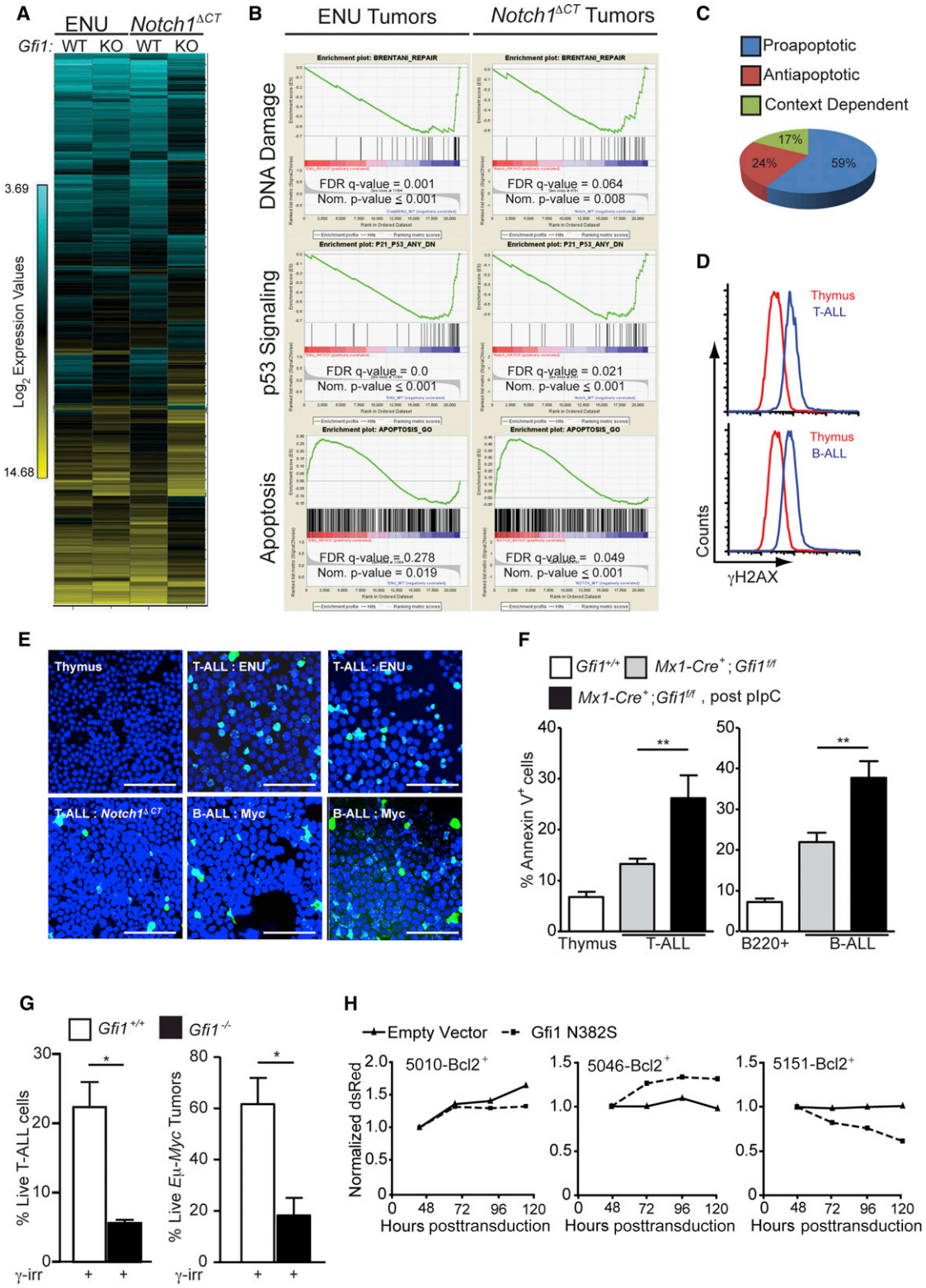

Figure 4. Gfi1 Mediates DNA Damage and p53 Signaling to Control Apoptosis

(A) Unsupervised hierarchical clustering of the averaged normalized Log_2 gene expression values from ENU (n = 3) or ENU/*Notch1*$^{\Delta CT}$ (n = 2)-induced T-ALL arising in *Gfi1*$^{f/f}$ (wild-type, WT) or *Mx1-Cre*$^{+}$*;Gfi1*$^{f/f}$ (knockout, KO) pIpC-treated mice (ENU WT, n = 3; ENU KO, n = 3; ENU/*Notch1*$^{\Delta CT}$ WT, n = 2; ENU/*Notch1*$^{\Delta CT}$ KO, n = 2).

(B) GSEA butterfly plots for pathways related to DNA damage, p53 signaling, or apoptosis found in both ENU- and *Notch1*$^{\Delta CT}$-initiated tumor signatures from (A).

(legend continued on next page)

mechanism demonstrated that Gfi1 and p53 can physically interact in transfected cells and in irradiated thymocytes (Figures 5H and 5I) and that Gfi1 was able to repress p53-mediated transcriptional activation of a model reporter gene (Figure 5J). Notably, methylation of p53 at K372 leads to increased stability of chromatin-bound p53 and to the activation of p53 target genes, whereas demethylation of K372 has an inhibitory effect on p53 (West and Gozani, 2011). Immunoprecipitation and immunoblot experiments with *Gfi1*$^{+/+}$ and *Gfi1*$^{-/-}$ thymocytes showed that absence of Gfi1 leads to a substantial increase of p53-K372me, regardless of irradiation (Figure 5K). Moreover, thymocytes from knockin mice expressing only a Gfi1^{P2A} mutant (Fiolka et al., 2006) that lacks the ability to bind LSD1 (Saleque et al., 2007) also displayed a substantial increase of p53-K372me (Figure 5L). These data suggest that Gfi1 restricts p53 activity through Gfi1 SNAG-dependent cofactor recruitment and p53 demethylation (Figure 5M).

Targeting GFI1 in Human ALL Leads to Tumor Death

To test whether Gfi1 could be a suitable target for therapy of human leukemia, we used human T-ALL cell lines and reduced Gfi1 expression either by transduction of previously described shRNA-expressing lentiviral vectors (Velu et al., 2009) or Vivo-Morpholinos (Morcos et al., 2008) specifically designed against *GFI1*. In both cases, reduction of Gfi1 impeded the growth of T-ALL cell lines, which correlated with a higher level of apoptosis (Figures 6A–6C and S5A–S5C), suggesting that T-ALL is sensitive to the induction of apoptosis. When we used the pan-Bcl2 inhibitors Obatoclax and ABT-263 on three independent T-ALL lines, we observed IC_{50} values approximately 10-fold lower than those observed in acute myeloid leukemia (AML), where the use of these drugs is currently in clinical trials (Figure 6D). Inhibition of Gfi1 further increased the efficiency of both Obatoclax treatment (Figure 6E) and radiation therapy (Figure S5D). To demonstrate the contribution of p53 to Gfi1 loss-of-function apoptosis, we used Vivo-Morpholinos to first antagonize p53 expression then Gfi1 expression. We observed a significant decrease in the ability of the Gfi1 Vivo-Morpholinos to induce apoptosis after p53 Vivo-Morpholino pretreatment (Figure S5E). Similar results were obtained using p53-targeting shRNA lentiviruses followed by Gfi1 Vivo-Morpholino treatment (data not shown).

Next, we examined Gfi1 inhibition in primary patient samples. Due to the significant limitations of in vitro systems to support primary T-ALL cell survival, we transplanted primary patient specimens into immune-deficient Nod/Scid/IL2R$\gamma^{-/-}$ (NSG) mice then tested whether targeting Gfi1 using morpholinos is a viable approach to treat leukemia. The cells were allowed to engraft and expand for 4 days before the mice were injected with Vivo-Morpholinos over a 3 week period and monitored for survival. Gfi1 Vivo-Morpholino-treated animals showed a trend toward increased survival after only three injections (Figures S5F–S5I). We repeated the assay with samples from a patient who failed to respond to current therapies but increased the treatment frequency. When control morpholino (NT)-treated mice became moribund, we analyzed the tissues of all of the transplanted mice for the presence of human T-ALL cells. Targeting Gfi1 significantly impeded the expansion of the human leukemia in the BM, peripheral blood, and the spleen of the transplanted NSG mice (Figures 6F–6H), whereas treatment of healthy mice with the same dosing regimen did not lead to adverse effects (Figure S5J).

DISCUSSION

Important roles for Gfi1 in normal lymphoid development and acceleration of murine T cell leukemia have previously been established (Blyth et al., 2001; Chakraborty et al., 2008; Dabrowska et al., 2009; Gilks et al., 1993; Scheijen et al., 1997; Schmidt et al., 1996; Uren et al., 2008; Yücel et al., 2003). Yet, questions remained whether Gfi1 was required for the development or maintenance of human lymphoid leukemia. In the current study, we found that ablation of Gfi1 leads to regression of already established murine lymphoid neoplasms occurring through the induction of p53-dependent apoptotic pathways. Our results indicate that leukemic cells in general require Gfi1 because the ablation of Gfi1 led to lymphoid tumor regression and host survival independently of the transforming pathway or tumor etiology. It is thus conceivable that Gfi1 is an "oncorequisite" factor, a normal cellular protein upon which malignant cells uniquely depend for their survival. This offers a different paradigm for cancer therapeutics and suggests that normal cellular proteins, independent of their mutation status in human tumors, can be excellent targets for clinical intervention.

Our findings are surprising given the recently identified function of Gfi1 in myeloproliferative disease (MPD) and AML, where Gfi1 loss of function derepresses HoxA9, Meis1, and Pbx1, and can cooperate with other oncogenic lesions to transform myeloid progenitors (Horman et al., 2009). Furthermore, a SNP in the human *GFI1* deregulates *HOXA9* expression and increases the risk for human AML by 60% (Khandanpour et al.,

(C) Classification of genes in the leading edge of the GSEA apoptosis signature in (B) as Proapoptotic, Antiapoptotic, or Context Dependent.
(D and E) Determination of γH2AX levels in normal tissue as well as in B and T cell leukemia by FACS (D) and immunofluorescence (E). One experiment was performed. Scale bars, 50 μm.
(F) Level of spontaneous apoptosis in the indicated tissues and tumors before and after *Gfi1* deletion. T-ALL: *Gfi1*$^{+/+}$, n = 4; *Gfi1*$^{f/f}$, n = 17; *Gfi1*$^{\Delta/\Delta}$, n = 5. B-ALL: *Gfi1*$^{+/+}$, n = 4; *Gfi1*$^{f/f}$, n = 13; *Gfi1*$^{\Delta/\Delta}$, n = 4.
(G) *Gfi1*$^{+/+}$ (n = 7), *Gfi1*$^{-/-}$ and *Gfi1*$^{f/\Delta}$ (one constitutive Gfi1 KO tumor and two tumors, in which Gfi1 has been deleted with more than 50% excision, n = 3), thymic tumor cells and *Gfi1*$^{+/+}$;*Eμ-Myc*$^{+}$ (n = 7), and *Gfi1*$^{-/-}$;*Eμ-Myc*$^{+}$ (n = 3) lymphomas were explanted and irradiated (6 Gy), and examined for Annexin V staining by FACS.
(H) T-ALL cell lines 5151, 5046, and 5010 were transduced with retrovirus vectors MSCV-Bcl-2, expanded, and then transduced with vectors encoding Gfi1^{N382S} and dsRed or dsRed alone. dsRed was measured over time by FACS and normalized to the level at 48 hr. One of three representative experiments is shown. Mean and mean ± SEM are shown unless stated otherwise. *$p < 0.05$, **$p < 0.01$.
See also Table S2.

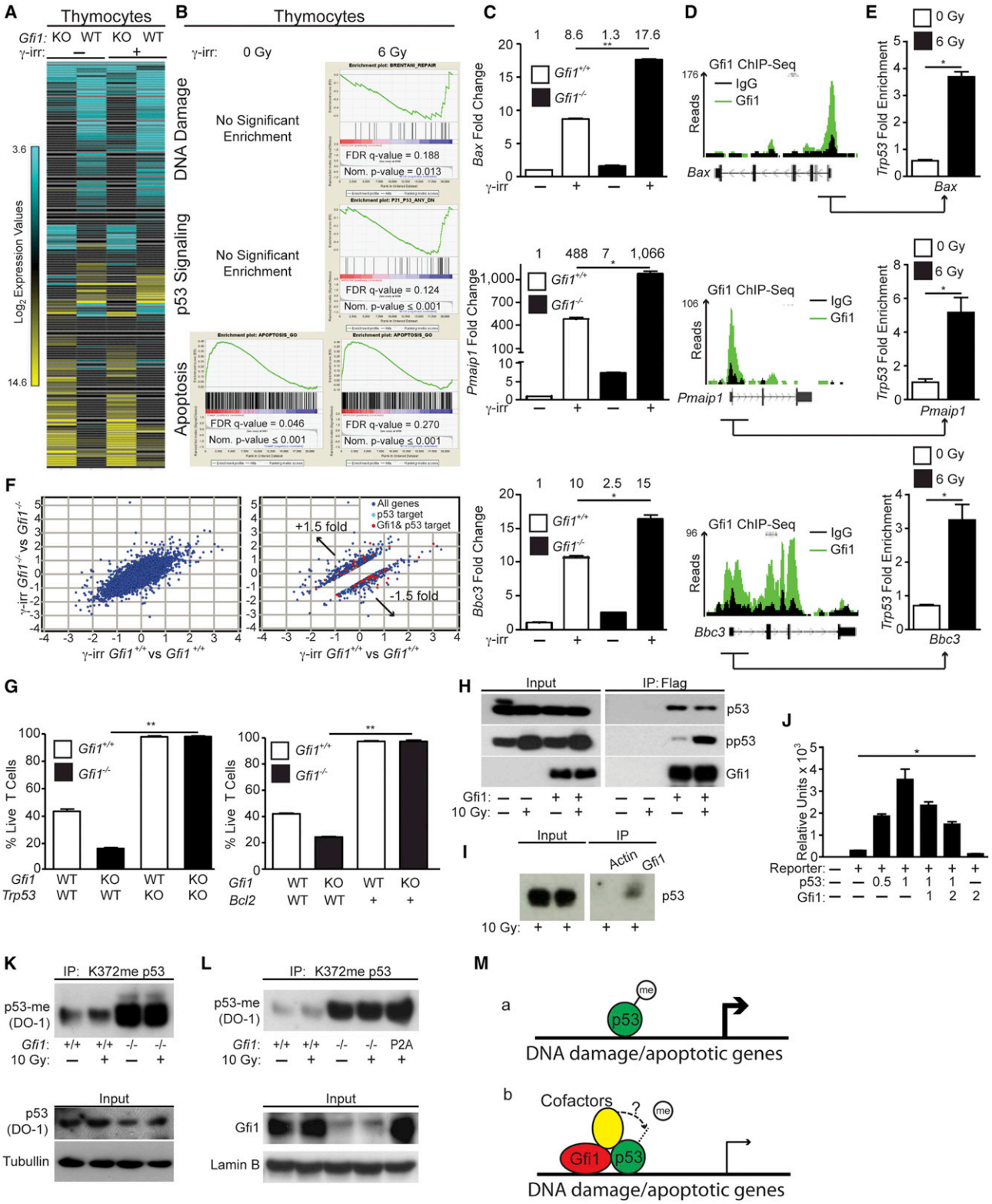

Figure 5. Gfi1 Restricts p53-Dependent Induction of Apoptosis

(A) Unsupervised hierarchical clustering of the averaged normalized Log_2 gene expression values from *Gfi1*$^{+/+}$ (WT) and *Gfi1*$^{-/-}$ (KO) thymocytes with or without irradiation (*Gfi1*$^{+/+}$ control, n = 2; *Gfi1*$^{-/-}$ control, n = 2; *Gfi1*$^{+/+}$ irradiated, n = 3; *Gfi1*$^{-/-}$ irradiated, n = 3).

(B) GSEA butterfly plots for pathways related to DNA damage, p53 signaling, or apoptosis enriched in Gfi1-deficient tumors (Figure 4B) that emerge in *Gfi1*$^{-/-}$ T cells only after irradiation.

(legend continued on next page)

2012); however, further experimentation is still necessary to incisively define a role for Gfi1 in human AML. HoxA9 signaling is present in mixed-lineage leukemia but is active in less than 10% of patients with T-ALL (Ferrando et al., 2002). Thus, patients with rare HoxA9-active T-ALL may not benefit from receiving Gfi1-targeting therapies. Therefore, careful molecular pathology will likely be important to stratify patients for Gfi1-targeted therapeutics.

Recent work suggested that oncogenic signaling in general causes uncoordinated cell division resulting in collapsed replication forks and the initiation of p53-dependent DNA damage responses causing cell death (Halazonetis et al., 2008; Bartek et al., 2007; Bartkova et al., 2007; Di Micco et al., 2006). Tumor cells have to counteract this "oncogenic stress" signal to avoid cell death, for instance by mutating *TP53*. However, *TP53* mutations are rare in T-ALL; hence, leukemic cells have to devise other measures to circumvent apoptosis. Our data offer an explanation as to how lymphoid malignancies can overcome p53 activation and why they are dependent on Gfi1. We propose that DNA damage, initiated by oncogenic stress during malignant transformation, induces p53 activity. High Gfi1-expressing subclones can thus be selected during transformation to enable global restriction of p53-mediated apoptosis. Gfi1 exerts this function by (1) co-occupying p53 target genes such as *Bax*, *Pmaip1*, and *Bbc3*; (2) binding to p53-bound transcriptional complexes; and (3) limiting the methylation of p53 at K372 thereby restricting the activity of p53 and the activation of p53 target genes.

The function of Gfi1 to limit p53-K372 methylation (p53-K369 in murine cells) (Kurash et al., 2008) appears to be dependent on its ability to bind SNAG-dependent cofactors such as LSD1. It is known that demethylation of p53 at K370 is mediated by LSD1 and prevents p53 association with coactivators such as p53BP1 (Huang et al., 2007). We propose that leukemic cells use a Gfi1-LSD1 or a Gfi1-SNAG-dependent cofactor complex to demethylate p53 at K372, which prevents a full activation of p53 and its proapoptotic target genes. However, we cannot exclude the possibility that loss of Gfi1-SNAG-dependent transcriptional repression leads to the activation of factors, which may directly affect p53 activation/methylation status. In either case, ablation of Gfi1 leads to an accumulation of more active methylated p53, to a more efficient transactivation of proapoptotic p53 target genes, and as a consequence, to accelerated cell death. Several independent lines of evidence support this notion including reporter gene assays, ChIP-seq data, biochemical analyses, and expression data and offer a mechanistic explanation why Gfi1 ablation leads to regression of murine lymphomas and causes an inhibition of primary human T-ALL cell expansion in immune-deficient mice.

Our findings have direct implications for current ALL treatments, which consist of chemotherapy and irradiation. Both are nonspecific and highly toxic, damaging host and tumor tissues. These therapies function mainly through the induction of DNA damage and the initiation of p53-dependent DNA damage response pathways that cause cell death. Even when effective, patients can suffer dramatic side effects from standard ALL treatments. Therefore, reducing chemotherapeutic or irradiation dose and thus their side effects while maintaining their efficacy would directly benefit patients. The main result from our study suggests that this goal can be achieved by inhibiting the function of Gfi1 in patients with T-ALL because ablation of Gfi1 accelerates p53-induced cell death in leukemic cells. According to our data, leukemic cells lacking Gfi1 will be more sensitive to DNA damage-inducing chemo- or irradiation therapy and undergo accelerated apoptosis. It is thus conceivable that targeting Gfi1 will not only significantly improve response rates but may in particular allow lower effective doses of chemotherapeutic agents or irradiation. In summary, our findings suggest that Gfi1 represents an Achilles' heel of lymphoid leukemias, and our approach to target Gfi1 may soon move to clinical trials.

(C) Expression of *Bax*, *Pmaip1* (*Noxa*), and *Bbc3* (*Puma*) in *Gfi1*$^{+/+}$ and *Gfi1*$^{-/-}$ thymocytes before and after irradiation. One representative experiment out of at least two experiments is shown. The numbers above the bars represent the mean values of the measurements.

(D) Peaks across the *Bax*, *Pmaip1*, and *Bbc3* loci from Gfi1 ChIP-seq of murine hematopoietic progenitor cells immortalized by retroviral transduction of an MLL-ENL expression vector (GSE31657).

(E) ChIP of p53 using primers from Gfi1-bound regions (underscored with arrow in D) of *Bax*, *Pmaip1*, and *Bbc3* before and after irradiation. Represented are the mean and SD of the fold difference compared to IgG control from one experiment with three technical repeats.

(F) Log_2 values of the fold change of the irradiated versus unirradiated gene expression values of all genes (left) or 1.5-fold differentially regulated (right) between *Gfi1*$^{+/+}$ and *Gfi1*$^{-/-}$ thymocytes. Gfi1-bound (identified in D) p53 target genes are shown in red.

(G) Percentage of live *Gfi1*$^{+/+}$;*Trp53*$^{+/+}$, *Gfi1*$^{-/-}$;*Trp53*$^{+/+}$, *Gfi1*$^{+/+}$;*Trp53*$^{-/-}$, and *Gfi1*$^{-/-}$;*Trp53*$^{-/-}$ thymocytes after ex vivo γ irradiation (left, n = 3). Percentage of live *Gfi1*$^{+/+}$, *Gfi1*$^{-/-}$, *Gfi1*$^{+/+}$;*Vav-Bcl2*, and *Gfi1*$^{-/-}$;*Vav-Bcl2* thymocytes after ex vivo γ irradiation (right, n = 3).

(H) Immunoblot of total-cell lysate (left) and immunoprecipitation (right) were performed using p53, phospho- p53, or Gfi1 antibodies on lysates from untreated or irradiated 293T cells transfected as indicated with FLAG-tagged Gfi1 constructs. One representative experiment from at least two experiments is shown.

(I) Immunoblot of total-cell lysate (left) and immunoprecipitation using either Gfi1 or an isotype control (actin) antibody (right) were performed using phospho-p53 (Ser15) antibody on lysates from irradiated thymocytes cells. One representative experiment from at least two experiments is shown.

(J) Reporter expression assay using the *Bax* promoter and various amounts (μg) of transfected vectors encoding p53 or Gfi1.

(K) Thymocytes from the indicated mice were irradiated or left untreated. After 30 min, total-cell lysates were immunoprecipitated with an anti-mono-methyl K372 p53 antibody, then immunoblotted with an anti-p53 antibody. p53 and tubulin in total-cell lysates are also shown. One experiment out of at least two experiments is shown.

(L) Thymocyte nuclear extracts from the indicated mouse strains were immunoprecipitated with an anti-mono-methyl K372 p53 antibody, then immunoblotted with an anti-p53 antibody. Input control shows the level of Gfi1 in thymocytes from *Gfi1*$^{+/+}$, *Gfi1*$^{-/-}$, and *Gfi1*$^{P2A/P2A}$ mice and the loading control LaminB. One experiment out of at least two experiments is shown.

(M) Schematic representation showing methylated p53 binds to DNA and robustly activates the expression of target genes (a), and Gfi1 co-occupancy of a subset of p53 targets tethers a Gfi1 SNAG-dependent cofactor, which demethylates p53 to dampen the expression of p53 target gene (b).

Mean and ± mean SEM are shown unless stated otherwise. *$p < 0.05$, **$p < 0.01$.

See also Figure S4.

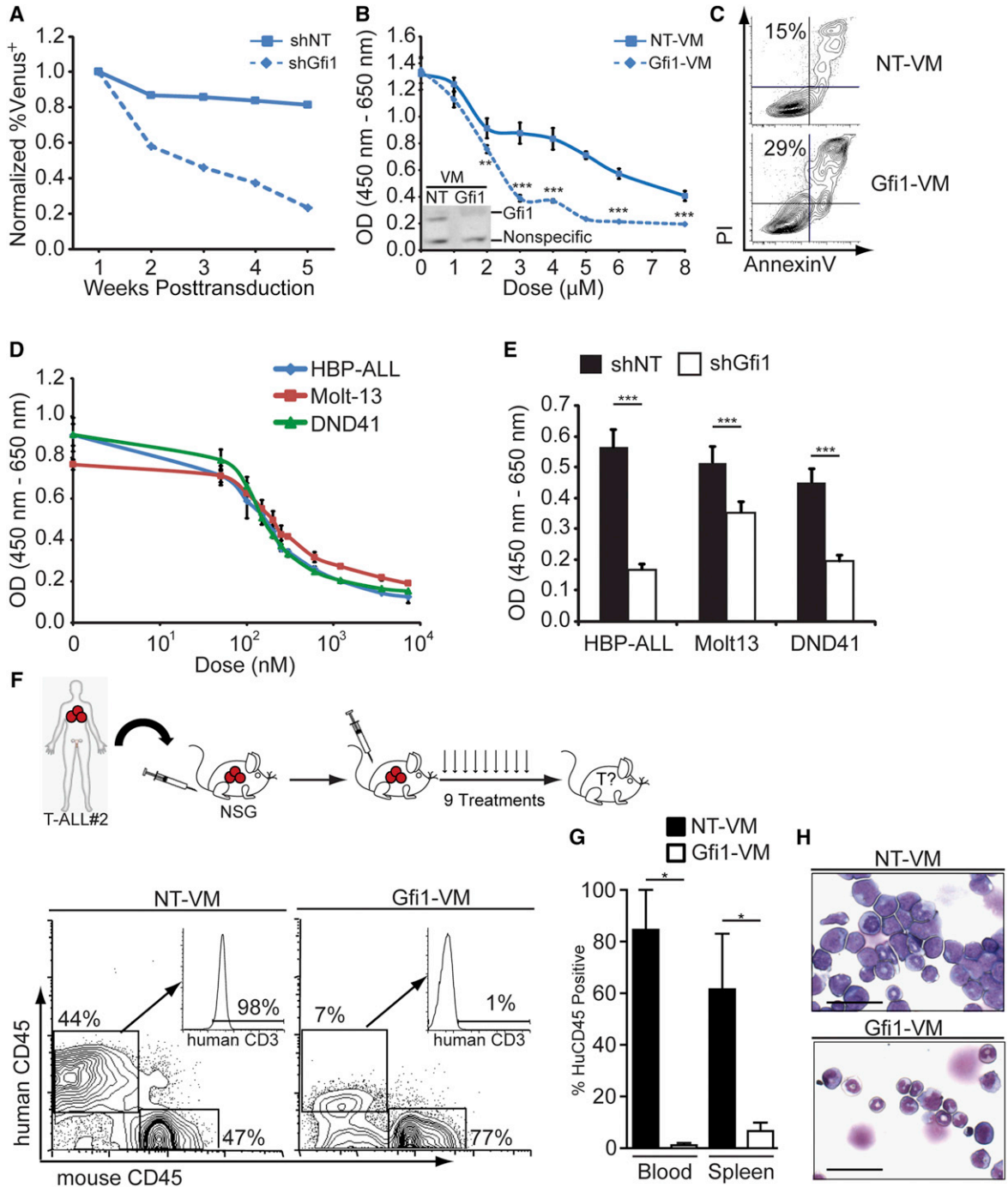

Figure 6. Gfi1 as a Target to Treat Human Leukemia

(A) HBP-ALL cells were transduced with Venus-marked shRNA-expressing lentiviral vectors targeting Gfi1 (shGfi1, dotted line) or nontargeting control (shNT, solid line). Expression of Venus was measured by FACS 72 hr posttransduction, which was set as 1, and subsequent measurements were taken by FACS over a 5 week period and normalized to the first reading, p = 0.058.

(B) Growth of HBP-ALL cells treated with Gfi1 or NT Vivo-Morpholinos (VM) as measured by WST assay for 48 hr. Inset shows immunoblot for Gfi1 in HBP-ALL cells treated with NT or Gfi1-VM (4 μM) for 16 hr.

(C) Annexin V and PI staining of HBP-ALL cells after 16 hr of Gfi1 or NT VM treatment (4 μM).

(D) Growth of T-ALL cell lines treated with indicated doses of the Obatoclax as measured by WST assay for 48 hr.

(E) Gfi1 knockdown was combined with Obatoclax treatment (200 nM), and growth was measured by WST assay for 48 hr. One representative experiment is shown; experiments were repeated two to three times (A–E).

(F) Top view shows primary patient T-ALL samples that were transplanted in NSG mice and then mice were injected with Gfi1 or NT VM three times per week for 3 weeks. Bottom view is a FACS analysis of human CD45 and human CD3 of NT (n = 2) or Gfi1-treated (n = 3) mice.

(legend continued on next page)

EXPERIMENTAL PROCEDURES

All other experimental procedures can be found in the Supplemental Information.

Mice

LckCre^{+}, *Mx1-Cre*$^{+}$, C57BL/6, CD45.1, *Trp53*$^{-/-}$, and NSG mice were obtained from The Jackson Laboratory (Bar Harbor, ME, USA). Regarding other mouse strains, please refer to the Supplemental Experimental Procedures. Mice were housed in either single ventilated cages with top filters or microisolator cages. The Institutional Animal Care, Use and Ethical Committees responsible for Cincinnati Children's Hospital Medical Center (CCHMC), the Institut de Recherches Cliniques de Montréal (IRCM), and University Clinic Essen (UKE) reviewed and approved all animal experimentation.

Xenograft Transplants and Morpholino Treatment

Diagnostic patient samples were obtained after informed consent according to Helsinki declaration and with approval from the institutional review boards at the IRCM, CCHMC, and UKE for the described experiments. One million T-ALL cells were transplanted (i.v.) into NSG mice that were injected 4 days later (i.v.) with Vivo-Morpholinos (Gene Tools) as described in Figures 6 and S5 with 25 nM of control ("NT-VM," 5′-CCTCTTACCTCAGTTACAATT TATA-3′) or Gfi1-specific ("Gfi1-VM," 5′-ATGGTGGTCCGGCACTTTCCCCACT-3′) Vivo-Morpholinos per injection.

In Vivo Deletion of Gfi1 and Ultrasound Observation

Gfi1$^{f/f}$ or *RosaCre*^{ERT2} *Gfi1*$^{f/f}$ mice were injected (i.p.) with 1 mg OHT (Sigma-Aldrich) dissolved in 100 μl of corn oil the first 5 days following transplantation. *Gfi1*$^{f/f}$ or *Mx1-Cre*$^{+}$;*Gfi1*$^{f/f}$ mice were either injected (i.p.) 4 weeks after the last ENU injection or 3 days after the transplantation of the tumor cells with 500 mg plpC (Sigma-Aldrich) seven times every other day. PCR validation of in vivo deletion was performed as previously described (Horman et al., 2009). Ultrasound observation was performed on anesthetized mice, and thymic tumors were measured using the Visualsonic ultrasound machine and the Vev0770 imaging software (Toronto). A tumor was called present if the thymic surface area measured in the horizontal and sagittal plane was larger than 8 mm^2 because average thymic surface of age-matched, untreated *Gfi1*$^{f/f}$ control mice is 4 mm^2, and if the tumor exhibited growth of more than 50% during the last 2 weeks of observation.

Statistics

GraphPad Prism software (GraphPad Software, La Jolla, CA, USA) was used for most statistical analysis. Kaplan-Meier curves were analyzed using log rank tests. A p value ≤ 0.05 was considered significant for all analyses. Differences in incidences of leukemia or lymphoma among the different groups were determined using Fisher's exact test. Two-tailed unpaired Student's t tests were used to calculate the differences in the gene expression of patient data, WBC, and spleen weights of transplanted mice, as well as the differences in cell number or tumors in ENU and MMLV-treated mice. The Mann-Whitney U test was used to determine significance in counterselection assays. Two-way ANOVAs were used to calculate significance of Vivo-Morpholino dose-responsive curves. Differences in Annexin V staining of *Bcl2*-transgenic *Gfi1*$^{-/-}$ mice and *Trp53p53*$^{-/-}$*Gfi1*$^{-/-}$ were calculated using one-way ANOVAs. GSEA FDR Q values <0.25 were used as a cutoff for enriched signatures.

ACCESSION NUMBERS

Array data are accessible under GEO accession number GSE32910.

SUPPLEMENTAL INFORMATION

Supplemental Information includes five figures, two tables, and Supplemental Experimental Procedures and can be found with this article online at http://dx.doi.org/10.1016/j.ccr.2013.01.011.

ACKNOWLEDGMENTS

We thank David Hildeman, Anil Jegga, Patrick Zweidler-McKay, Michelle Kelliher, Tom Look, and Paul Jolicouer for expertise and for kindly providing plasmids, cell lines, reagents, and mice. C.K. was supported by a fellowship of the Cole Foundation, the IFZ fellowship of the University Clinic of Essen, and a Max-Eder fellowship from the German Cancer fund. J.D.P. is a Pelotonia Fellow and was supported by the University of Cincinnati Cancer Therapeutics T32 training grant (T32-CA117846). J.S. was supported by a Gordon Piller PhD studentship from Leukaemia and Lymphoma Research UK, S.R.H. by a fellowship from CancerFree Kids, and J.Z. and W.E.P. by the Division of Intramural Research, National Institute of Allergy and Infectious Diseases. H.L.G. was supported by the Leukemia and Lymphoma Society of America, NIH CA105152, CA159845, Alex's Lemonade Stand, and thanks the Center of Excellence in Molecular Hematology P30 award (DK090971). T.M. was supported by a Canada Research Chair (Tier 1) and grants from the Canadian Institutes of Health Research (CIHR, MOP-84238, MOP-111011). C.K. and J.D.P. designed and performed experiments, analyzed data, and wrote the manuscript. M.-C.G., L.V., J.S., R.C., S.R.H., J.K., and B.G. performed experiments and assisted analyses. J.Z. and W.E.P. provided the *Gfi1*$^{f/f}$ mouse strain. U.D. provided funding and oversaw research. H.L.G. and T.M. were responsible for concept and design of experiments, oversaw research, wrote the manuscript, and provided funding.

Received: December 22, 2011
Revised: September 11, 2012
Accepted: January 18, 2013
Published: February 11, 2013

REFERENCES

Adams, J.M., Harris, A.W., Pinkert, C.A., Corcoran, L.M., Alexander, W.S., Cory, S., Palmiter, R.D., and Brinster, R.L. (1985). The c-myc oncogene driven by immunoglobulin enhancers induces lymphoid malignancy in transgenic mice. Nature *318*, 533–538.

Bartek, J., Bartkova, J., and Lukas, J. (2007). DNA damage signalling guards against activated oncogenes and tumour progression. Oncogene *26*, 7773–7779.

Bartkova, J., Horejsí, Z., Sehested, M., Nesland, J.M., Rajpert-De Meyts, E., Skakkebaek, N.E., Stucki, M., Jackson, S., Lukas, J., and Bartek, J. (2007). DNA damage response mediators MDC1 and 53BP1: constitutive activation and aberrant loss in breast and lung cancer, but not in testicular germ cell tumours. Oncogene *26*, 7414–7422.

Blyth, K., Terry, A., Mackay, N., Vaillant, F., Bell, M., Cameron, E.R., Neil, J.C., and Stewart, M. (2001). Runx2: a novel oncogenic effector revealed by in vivo complementation and retroviral tagging. Oncogene *20*, 295–302.

Chakraborty, J., Okonta, H., Bagalb, H., Lee, S.J., Fink, B., Changanamkandat, R., and Duggan, J. (2008). Retroviral gene insertion in breast milk mediated lymphomagenesis. Virology *377*, 100–109.

Coustan-Smith, E., Mullighan, C.G., Onciu, M., Behm, F.G., Raimondi, S.C., Pei, D., Cheng, C., Su, X., Rubnitz, J.E., Basso, G., et al. (2009). Early T-cell precursor leukaemia: a subtype of very high-risk acute lymphoblastic leukaemia. Lancet Oncol. *10*, 147–156.

(G) Quantification of total human CD45^{+} cells in the blood and spleen from mice in (F).
(H) Cytospins of the BM from mice in (F). Scale bars, 50 μm.
Mean and mean ± SEM are shown unless stated otherwise. *p < 0.05, **p < 0.01, ***p < 0.001.
See also Figure S5.

Cullion, K., Draheim, K.M., Hermance, N., Tammam, J., Sharma, V.M., Ware, C., Nikov, G., Krishnamoorthy, V., Majumder, P.K., and Kelliher, M.A. (2009). Targeting the Notch1 and mTOR pathways in a mouse T-ALL model. Blood *113*, 6172–6181.

Dabrowska, M.J., Dybkaer, K., Johnsen, H.E., Wang, B., Wabl, M., and Pedersen, F.S. (2009). Loss of MicroRNA targets in the 3′ untranslated region as a mechanism of retroviral insertional activation of growth factor independence 1. J. Virol. *83*, 8051–8061.

Di Micco, R., Fumagalli, M., Cicalese, A., Piccinin, S., Gasparini, P., Luise, C., Schurra, C., Garre', M., Nuciforo, P.G., Bensimon, A., et al. (2006). Oncogene-induced senescence is a DNA damage response triggered by DNA hyper-replication. Nature *444*, 638–642.

Ferrando, A.A., Neuberg, D.S., Staunton, J., Loh, M.L., Huard, C., Raimondi, S.C., Behm, F.G., Pui, C.H., Downing, J.R., Gilliland, D.G., et al. (2002). Gene expression signatures define novel oncogenic pathways in T cell acute lymphoblastic leukemia. Cancer Cell *1*, 75–87.

Fiolka, K., Hertzano, R., Vassen, L., Zeng, H., Hermesh, O., Avraham, K.B., Dührsen, U., and Möröy, T. (2006). Gfi1 and Gfi1b act equivalently in haematopoiesis, but have distinct, non-overlapping functions in inner ear development. EMBO Rep. *7*, 326–333.

Gilks, C.B., Bear, S.E., Grimes, H.L., and Tsichlis, P.N. (1993). Progression of interleukin-2 (IL-2)-dependent rat T cell lymphoma lines to IL-2-independent growth following activation of a gene (Gfi-1) encoding a novel zinc finger protein. Mol. Cell. Biol. *13*, 1759–1768.

Gökbuget, N., and Hoelzer, D. (2009). Treatment of adult acute lymphoblastic leukemia. Semin. Hematol. *46*, 64–75.

Halazonetis, T.D., Gorgoulis, V.G., and Bartek, J. (2008). An oncogene-induced DNA damage model for cancer development. Science *319*, 1352–1355.

Hameyer, D., Loonstra, A., Eshkind, L., Schmitt, S., Antunes, C., Groen, A., Bindels, E., Jonkers, J., Krimpenfort, P., Meuwissen, R., et al. (2007). Toxicity of ligand-dependent Cre recombinases and generation of a conditional Cre deleter mouse allowing mosaic recombination in peripheral tissues. Physiol. Genomics *31*, 32–41.

Horman, S.R., Velu, C.S., Chaubey, A., Bourdeau, T., Zhu, J., Paul, W.E., Gebelein, B., and Grimes, H.L. (2009). Gfi1 integrates progenitor versus granulocytic transcriptional programming. Blood *113*, 5466–5475.

Huang, J., Sengupta, R., Espejo, A.B., Lee, M.G., Dorsey, J.A., Richter, M., Opravil, S., Shiekhattar, R., Bedford, M.T., Jenuwein, T., and Berger, S.L. (2007). p53 is regulated by the lysine demethylase LSD1. Nature *449*, 105–108.

Khandanpour, C., Krongold, J., Schütte, J., Bouwman, F., Vassen, L., Gaudreau, M.C., Chen, R., Calero-Nieto, F.J., Diamanti, E., Hannah, R., et al. (2012). The human GFI136N variant induces epigenetic changes at the Hoxa9 locus and accelerates K-RAS driven myeloproliferative disorder in mice. Blood *120*, 4006–4017.

Kundu, M., Compton, S., Garrett-Beal, L., Stacy, T., Starost, M.F., Eckhaus, M., Speck, N.A., and Liu, P.P. (2005). Runx1 deficiency predisposes mice to T-lymphoblastic lymphoma. Blood *106*, 3621–3624.

Kurash, J.K., Lei, H., Shen, Q., Marston, W.L., Granda, B.W., Fan, H., Wall, D., Li, E., and Gaudet, F. (2008). Methylation of p53 by Set7/9 mediates p53 acetylation and activity in vivo. Mol. Cell *29*, 392–400.

Li, H., Ji, M., Klarmann, K.D., and Keller, J.R. (2010). Repression of Id2 expression by Gfi-1 is required for B-cell and myeloid development. Blood *116*, 1060–1069.

Margolin, A.A., Palomero, T., Sumazin, P., Califano, A., Ferrando, A.A., and Stolovitzky, G. (2009). ChIP-on-chip significance analysis reveals large-scale binding and regulation by human transcription factor oncogenes. Proc. Natl. Acad. Sci. USA *106*, 244–249.

Medyouf, H., Gusscott, S., Wang, H., Tseng, J.C., Wai, C., Nemirovsky, O., Trumpp, A., Pflumio, F., Carboni, J., Gottardis, M., et al. (2011). High-level IGF1R expression is required for leukemia-initiating cell activity in T-ALL and is supported by Notch signaling. J. Exp. Med. *208*, 1809–1822.

Morcos, P.A., Li, Y., and Jiang, S. (2008). Vivo-Morpholinos: a non-peptide transporter delivers Morpholinos into a wide array of mouse tissues. Biotechniques *45*, 613–614, 616, 618 passim.

Murtaugh, L.C., Stanger, B.Z., Kwan, K.M., and Melton, D.A. (2003). Notch signaling controls multiple steps of pancreatic differentiation. Proc. Natl. Acad. Sci. USA *100*, 14920–14925.

O'Neil, J., Grim, J., Strack, P., Rao, S., Tibbitts, D., Winter, C., Hardwick, J., Welcker, M., Meijerink, J.P., Pieters, R., et al. (2007). FBW7 mutations in leukemic cells mediate NOTCH pathway activation and resistance to gamma-secretase inhibitors. J. Exp. Med. *204*, 1813–1824.

Palomero, T., Lim, W.K., Odom, D.T., Sulis, M.L., Real, P.J., Margolin, A., Barnes, K.C., O'Neil, J., Neuberg, D., Weng, A.P., et al. (2006). NOTCH1 directly regulates c-MYC and activates a feed-forward-loop transcriptional network promoting leukemic cell growth. Proc. Natl. Acad. Sci. USA *103*, 18261–18266.

Pargmann, D., Yücel, R., Kosan, C., Saba, I., Klein-Hitpass, L., Schimmer, S., Heyd, F., Dittmer, U., and Möröy, T. (2007). Differential impact of the transcriptional repressor Gfi1 on mature CD4+ and CD8+ T lymphocyte function. Eur. J. Immunol. *37*, 3551–3563.

Person, R.E., Li, F.Q., Duan, Z., Benson, K.F., Wechsler, J., Papadaki, H.A., Eliopoulos, G., Kaufman, C., Bertolone, S.J., Nakamoto, B., et al. (2003). Mutations in proto-oncogene GFI1 cause human neutropenia and target ELA2. Nat. Genet. *34*, 308–312.

Priceputu, E., Bouallaga, I., Zhang, Y., Li, X., Chrobak, P., Hanna, Z.S., Poudrier, J., Kay, D.G., and Jolicoeur, P. (2006). Structurally distinct ligand-binding or ligand-independent Notch1 mutants are leukemogenic but affect thymocyte development, apoptosis, and metastasis differently. J. Immunol. *177*, 2153–2166.

Saleque, S., Kim, J., Rooke, H.M., and Orkin, S.H. (2007). Epigenetic regulation of hematopoietic differentiation by Gfi-1 and Gfi-1b is mediated by the cofactors CoREST and LSD1. Mol. Cell *27*, 562–572.

Scheijen, B., Jonkers, J., Acton, D., and Berns, A. (1997). Characterization of pal-1, a common proviral insertion site in murine leukemia virus-induced lymphomas of c-myc and Pim-1 transgenic mice. J. Virol. *71*, 9–16.

Schmidt, T., Zörnig, M., Beneke, R., and Möröy, T. (1996). MoMuLV proviral integrations identified by Sup-F selection in tumors from infected myc/pim bitransgenic mice correlate with activation of the gfi-1 gene. Nucleic Acids Res. *24*, 2528–2534.

Schmidt, T., Karsunky, H., Gau, E., Zevnik, B., Elsässer, H.P., and Möröy, T. (1998). Zinc finger protein GFI-1 has low oncogenic potential but cooperates strongly with pim and myc genes in T-cell lymphomagenesis. Oncogene *17*, 2661–2667.

Sharma, V.M., Calvo, J.A., Draheim, K.M., Cunningham, L.A., Hermance, N., Beverly, L., Krishnamoorthy, V., Bhasin, M., Capobianco, A.J., and Kelliher, M.A. (2006). Notch1 contributes to mouse T-cell leukemia by directly inducing the expression of c-myc. Mol. Cell. Biol. *26*, 8022–8031.

Spooner, C.J., Cheng, J.X., Pujadas, E., Laslo, P., and Singh, H. (2009). A recurrent network involving the transcription factors PU.1 and Gfi1 orchestrates innate and adaptive immune cell fates. Immunity *31*, 576–586.

Subramanian, A., Tamayo, P., Mootha, V.K., Mukherjee, S., Ebert, B.L., Gillette, M.A., Paulovich, A., Pomeroy, S.L., Golub, T.R., Lander, E.S., and Mesirov, J.P. (2005). Gene set enrichment analysis: a knowledge-based approach for interpreting genome-wide expression profiles. Proc. Natl. Acad. Sci. USA *102*, 15545–15550.

Thompson, B.J., Buonamici, S., Sulis, M.L., Palomero, T., Vilimas, T., Basso, G., Ferrando, A., and Aifantis, I. (2007). The SCFFBW7 ubiquitin ligase complex as a tumor suppressor in T cell leukemia. J. Exp. Med. *204*, 1825–1835.

Uren, A.G., Kool, J., Matentzoglu, K., de Ridder, J., Mattison, J., van Uitert, M., Lagcher, W., Sie, D., Tanger, E., Cox, T., et al. (2008). Large-scale mutagenesis in p19(ARF)- and p53-deficient mice identifies cancer genes and their collaborative networks. Cell *133*, 727–741.

Van Vlierberghe, P., van Grotel, M., Tchinda, J., Lee, C., Beverloo, H.B., van der Spek, P.J., Stubbs, A., Cools, J., Nagata, K., Fornerod, M., et al. (2008).

The recurrent SET-NUP214 fusion as a new HOXA activation mechanism in pediatric T-cell acute lymphoblastic leukemia. Blood *111*, 4668–4680.

Velu, C.S., Baktula, A.M., and Grimes, H.L. (2009). Gfi1 regulates miR-21 and miR-196b to control myelopoiesis. Blood *113*, 4720–4728.

Weng, A.P., Ferrando, A.A., Lee, W., Morris, J.P., 4th, Silverman, L.B., Sanchez-Irizarry, C., Blacklow, S.C., Look, A.T., and Aster, J.C. (2004). Activating mutations of NOTCH1 in human T cell acute lymphoblastic leukemia. Science *306*, 269–271.

Weng, A.P., Millholland, J.M., Yashiro-Ohtani, Y., Arcangeli, M.L., Lau, A., Wai, C., Del Bianco, C., Rodriguez, C.G., Sai, H., Tobias, J., et al. (2006). c-Myc is an important direct target of Notch1 in T-cell acute lymphoblastic leukemia/lymphoma. Genes Dev. *20*, 2096–2109.

West, L.E., and Gozani, O. (2011). Regulation of p53 function by lysine methylation. Epigenomics *3*, 361–369.

Yuan, Y., Zhou, L., Miyamoto, T., Iwasaki, H., Harakawa, N., Hetherington, C.J., Burel, S.A., Lagasse, E., Weissman, I.L., Akashi, K., and Zhang, D.E. (2001). AML1-ETO expression is directly involved in the development of acute myeloid leukemia in the presence of additional mutations. Proc. Natl. Acad. Sci. USA *98*, 10398–10403.

Yücel, R., Karsunky, H., Klein-Hitpass, L., and Möröy, T. (2003). The transcriptional repressor Gfi1 affects development of early, uncommitted c-Kit+ T cell progenitors and CD4/CD8 lineage decision in the thymus. J. Exp. Med. *197*, 831–844.

Zarebski, A., Velu, C.S., Baktula, A.M., Bourdeau, T., Horman, S.R., Basu, S., Bertolone, S.J., Horwitz, M., Hildeman, D.A., Trent, J.O., and Grimes, H.L. (2008). Mutations in growth factor independent-1 associated with human neutropenia block murine granulopoiesis through colony stimulating factor-1. Immunity *28*, 370–380.

Zhu, J., Jankovic, D., Grinberg, A., Guo, L., and Paul, W.E. (2006). Gfi-1 plays an important role in IL-2-mediated Th2 cell expansion. Proc. Natl. Acad. Sci. USA *103*, 18214–18219.

Zörnig, M., Schmidt, T., Karsunky, H., Grzeschiczek, A., and Möröy, T. (1996). Zinc finger protein GFI-1 cooperates with myc and pim-1 in T-cell lymphomagenesis by reducing the requirements for IL-2. Oncogene *12*, 1789–1801.